ELSEVIER

Journal of Photochemistry and Photobiology A: Chemistry 100 (1996) 77–84

Journal of PHOTOCHEMISTRY AND PHOTOBIOLOGY A: CHEMISTRY

Comparison of the photophysics of an aggregating and non-aggregating aluminium phthalocyanine system incorporated into unilamellar vesicles

S. Dhami, D. Phillips *

Department of Chemistry, Imperial College of Science, Technology and Medicine, Exhibition Road, South Kensington, London SW7 2AY, UK

Received 28 May 1996; accepted 18 June 1996

Abstract

The hydrophobic sensitizer, aluminium phthalocyanine chloride (AlPcCl), and the amphiphilic sensitizer, *cis*-disulphonated aluminium phthalocyanine (*cis*-$AlPcS_2$), were incorporated into small unilamellar vesicles (SUVs) and large unilamellar vesicles (LUVs). AlPcCl exhibits aggregation, which increases with increasing sensitizer concentration, whereas *cis*-$AlPcS_2$ is monomeric at all concentrations studied. Complex fluorescence decays are observed, showing decay time distributions which broaden with increasing phthalocyanine concentration. The phthalocyanine aggregate, although non-fluorescent, influences the overall photophysical behaviour of the phthalocyanine–vesicle system. The effect of aggregation on the resulting photophysics of phthalocyanines was investigated by comparing aggregated and non-aggregated phthalocyanine systems. The implications for photodynamic therapy (PDT) are briefly discussed.

Keywords: Aggregates; Aluminium phthalocyanine; Photophysics; Unilamellar vesicles

1. Introduction

Extensive studies have been carried out on phthalocyanines and their possible use as photodynamic therapy (PDT) agents [1–5]. In homogeneous solutions, the probability and efficiency of the photosensitization process depend on various photophysical parameters, such as the yield of the excited triplet state and its rate of decay. However, in microheterogeneous environments such as biological systems, e.g. cells and tissues, structural and functional parameters are also involved in determining the overall efficiency of the photosensitization process. These parameters regulate the uptake, localization and binding/interaction of the sensitizer molecules with the target molecules. The first step in the photosensitization of a cell is the binding of the sensitizer to the plasma membrane or permeation through the plasma membrane. In principle, permeation can occur by diffusion, by an active transport system or by endocytosis. Passive processes, such as diffusion and osmosis, result from concentration differences of substances inside and outside the cell, i.e. the movement of a substance down a concentration gradient. Active transport processes involve the movement of substances across a cell membrane against a potential gradient. The process usually involves carrier molecules. The process of endocytosis involves the formation of vesicles by the enfolding of a portion of the cell membrane, thus engulfing the sensitizer. The pouch that results then breaks loose from the outer portion of the membrane to form a vacuole, inside the cell, which fuses with a lysosome to form a secondary lysosome.

Phthalocyanines can be divided into two broad classes: water-soluble phthalocyanines, which can be injected directly into the bloodstream, and hydrophobic phthalocyanines, which must be administered using some type of delivery system. Thus the way in which the sensitizer is presented to the cell is also important, i.e. whether it is present in solution or bound to (lipo)proteins or delivered with special systems such as antibodies or liposomes. Following administration, the sensitizer is distributed throughout the cells. The final localization therefore depends on the type of cell, the delivery system, the physicochemical properties of the sensitizer molecules and the environment. The final site of localization of the sensitizer will also influence the overall efficiency of the photodynamic process. For both type I and type II processes, the sensitizer must localize at or near the site of photosensitization. This is because, in electron transfer reactions, an interaction between the target and sensitizing molecule is necessary and, in energy transfer reactions, the generated singlet oxygen has a definite lifetime. In addition, dyes which aggregate are not very good sensitizers as there is efficient energy transfer between the aggregated molecules. However,

* Corresponding author.

PII S1010-6030(96)04438-3

when bound to membranes, such dyes may monomerize and can very often efficiently induce photodynamic damage.

For the reasons described above, direct extrapolation of the results obtained from photophysical studies of sensitizers in homogeneous environments to the photodynamic behaviour of sensitizers observed in biological systems is very difficult. Therefore it is important to characterize the photophysical properties of sensitizers incorporated into microheterogeneous systems, such as liposomes. The hydrophobic/hydrophilic character of a sensitizer will determine its localization and thus the resulting photophysical properties in microheterogeneous systems. For example, hydrophobic sensitizers will be confined within the phospholipid bilayers of vesicles. Therefore the actual volume available is only a small fraction of the whole medium, and the local concentration of the sensitizer can be orders of magnitude larger than the concentration expected in a homogeneous environment. This may result in various intermolecular interactions. Photophysical studies of porphyrins [6] and phthalocyanines [7–10] in liposomal systems have been reported. In all cases, complex fluorescence decays were observed. These were either interpreted as being due to fluorescence from sensitizer dimers or aggregates or a result of sensitizer localization in more than one microenvironment within the liposomal dispersions.

In this study, the hydrophobic sensitizer, aluminium phthalocyanine chloride (AlPcCl), and the amphiphilic sensitizer, *cis*-disulphonated aluminium phthalocyanine (*cis*-$AlPcS_2$), were incorporated into small unilamellar vesicles (SUVs) (diameter, 52 nm) and large unilamellar vesicles (LUVs) (diameter, 84 nm) of DL-α-dipalmitoyl-phosphatidylcholine (DPPC). From the absorption spectra, it can be seen that *cis*-$AlPcS_2$ does not aggregate at all sensitizer concentrations, whereas AlPcCl exhibits aggregation at the higher concentrations. The photophysical properties of the aggregating and non-aggregating systems are compared, and the possible implications of these observations for PDT are briefly discussed.

2. Materials and methods

2.1. Materials

AlPcCl, purchased from Eastman Kodak, was used as received; *cis*-$AlPcS_2$ was prepared according to Ref. [11]. The cis isomer, which is the α,α-disubstituted regioisomer with the sulphonate groups on adjacent isoindole units, was isolated using reverse phase high performance liquid chromatography (HPLC) [12]. DPPC was purchased from Sigma. The buffer used was 0.01 M Tris–HCl (Tris, tris-(hydroxymethyl)aminomethane) (Aldrich) with 0.1 M sodium chloride (Aldrich), pH 7.4.

2.2. Preparation of unilamellar vesicles

The liposome dispersions were prepared by the injection method of Kremer et al. [13]. This procedure allows the preparation of unilamellar vesicles of pre-determined size through the injection of an ethanolic solution having different phospholipid concentrations into an aqueous buffered solution. The desired phthalocyanine concentrations in the liposomes were obtained by adding suitable volumes of a stock (1 mM) pyridine solution of the sensitizer to the ethanolic DPPC solution. The injection was performed at 55 °C with magnetic stirring and at a speed of 1 $\mu l\ s^{-1}$. The system was then allowed to cool to room temperature and was passed through a 450 nm Millipore filter. The organic solvents were eliminated by dialysing the liposome aqueous dispersion at 4 °C against 250 ml of Tris buffer for 2 h with one change of the buffer after the first hour. Dialysis tubing was sterilized in EDTA–bicarbonate solution (EDTA, ethylenediaminetetraacetic acid) prior to use. After preparation, all solutions were stored in the dark at 3–4 °C. SUVs of 26 nm radius (as estimated by electron microscopy [14]) and LUVs of 42 nm radius of DPPC were prepared starting from 9.5 mM or 32 mM phospholipid solution in absolute ethanol.

2.3. Methods

Absorption spectra were recorded with a Lambda 2 Perkin–Elmer spectrophotometer. Corrected fluorescence emission spectra (excitation at 610 nm) were obtained with a Spex Fluoromax spectrofluorometer. All fluorescence measurements were made with solutions with absorbance values of less than 0.1 at the maximum absorption by diluting the liposome dispersions with buffer in order to minimize distortions arising from the inner filter effect [15]. Fluorescence quantum yields are reported relative to chlorophyll *a* in ether ($\Phi_f = 0.32 \pm 0.05$) [16] and $AlPcS_2$ in methanol ($\Phi_f = 0.60 \pm 0.05$) [17].

Fluorescence decay times were recorded using the technique of time-correlated single-photon counting [18]. Excitation was provided by a frequency-doubled, mode-locked Nd:YAG laser (Coherent, Antares 76S), synchronously pumping a cavity-dumped dye laser (Coherent/590-03/7220), producing a 3.8 MHz train of pulses of less than 15 ps at 610 nm. The fluorescence was collected at 90° and passed through a polarizing filter set at the magic angle, and the wavelength was selected by a monochromator. A Hamamatsu R1564-U01 microchannel plate was used to detect the fluorescence, together with standard discriminators, time-to-amplitude converter and multichannel analyser, giving typical instrument response times of 50 ps full width at half-maximum (FWHM).

All decays were recorded to a minimum of 20 000 counts in the channel of maximum intensity and analysed by a non-linear least-squares iterative reconvolution fitting procedure (Glife, in-house software). Decays were also analysed globally, with two decay times common to each decay [19]. They

were also analysed using a decay time distribution analysis based on the maximum entropy method (MEM) [20] (Photon Technology International Maximum Entropy Analysis software). In all cases, the weighted residuals, their autocorrelation function and reduced chi-square were used to judge the quality of the fit [18].

Triplet state studies were carried out using a nanosecond flash photolysis system developed by Beeby et al. [21]. A 250 W xenon arc lamp was used to provide the analysing light. The excitation pulse was provided by an XeCl excimer laser (Lambda Physik FL2002) pumping a dye laser (Lambda Physik FL3002). A pump wavelength of 670 nm was used with typical energies of 10–500 μJ per pulse. The signal of the detector was displayed, averaged and digitized by a Tektronix 2432A oscilloscope. It was then transferred via an RS 232 interface to a personal computer where it was processed. Quantum yields Φ_t were determined by the comparative method using $AlPcS_2$ in methanol ($\Phi_t = 0.24$, ϵ_t(490 nm) = 36 000 mol^{-1} dm^3 cm^{-1}) [22] and water ($\Phi_t = 0.17$, ϵ_t(490 nm) = 36 000 mol^{-1} dm^3 cm^{-1}) [22].

All studies were carried out at 22 °C, which is below the phase transition temperature of the DPPC phospholipid (41.5 °C). The liposomes were therefore in a quasi-solid state, restricting the motility of the incorporated sensitizer.

3. Results

3.1. AlPcCl in small and large unilamellar vesicles

3.1.1. Steady state measurements

The absorption spectra of AlPcCl in SUVs and LUVs with varying sensitizer concentration are shown in Fig. 1 and Fig. 2 respectively. In both cases, a grow-in of the absorption at approximately 640 nm is observed at the higher sensitizer concentrations, indicating dimerization/aggregation of the phthalocyanine. The extent of aggregation is greater in the SUVs than in the LUVs. The corresponding Beer–Lambert plots are shown in Fig. 3. In both cases, non-linearity is observed, indicating sensitizer aggregation. The fluorescence quantum yields (Φ_f) are shown in Table 1. These values are

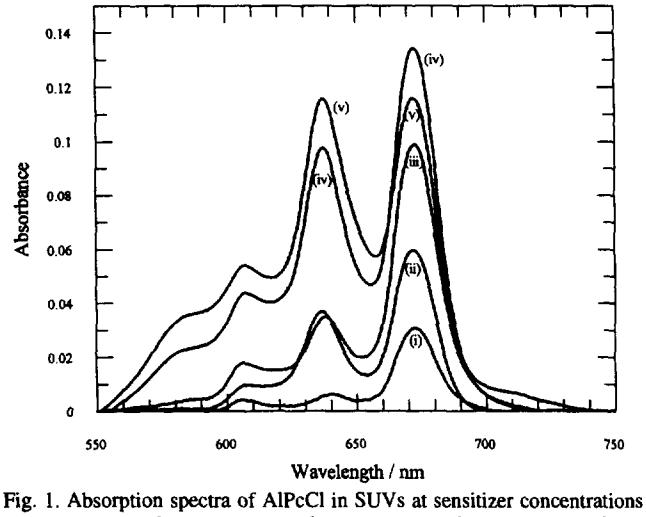

Fig. 1. Absorption spectra of AlPcCl in SUVs at sensitizer concentrations of (i) 0.30×10^{-6}, (ii) 0.83×10^{-6}, (iii) 1.5×10^{-6}, (iv) 5.4×10^{-6} and (v) 7.2×10^{-6} mol dm^{-3}.

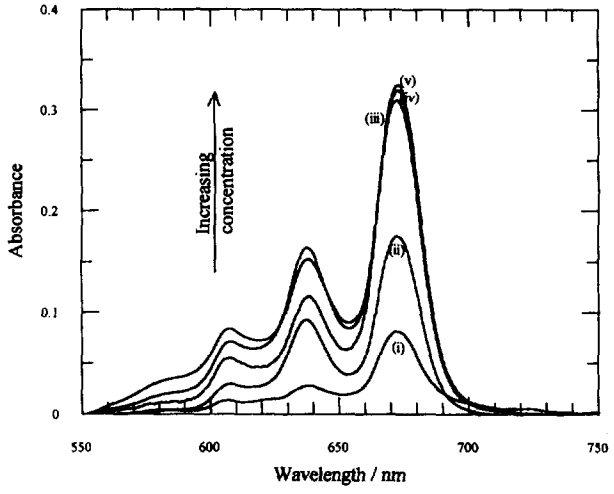

Fig. 2. Absorption spectra of AlPcCl in LUVs at sensitizer concentrations of (i) 0.87×10^{-6}, (ii) 2.7×10^{-6}, (iii) 4.3×10^{-6}, (iv) 6.3×10^{-6} and (v) 9.0×10^{-6} mol dm^{-3}.

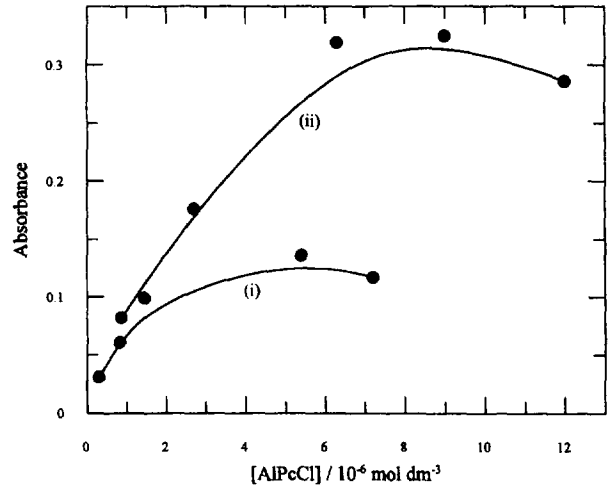

Fig. 3. Variation in the maximum absorbance (673 nm) as a function of the stoichiometric AlPcCl concentration in aqueous dispersions of DPPC SUVs (i) and LUVs (ii).

Table 1
Dependence of fluorescence quantum yields (Φ_f) on AlPcCl concentration in DPPC SUVs and LUVs

SUVs		LUVs	
[AlPcCl] (μM)	Φ_f^a	[AlPcCl] (μM)	Φ_f^a
0.30	0.34	0.87	0.40
0.83	0.28	2.70	0.26
1.45	0.16	6.30	0.22
5.40	0.09	9.00	0.16
7.20	0.07	12.00	0.09

[a] Φ_f not corrected for any dimer/aggregate absorption at the excitation wavelength (610 nm).

only estimates of the true values as it is difficult to correct for aggregate absorption at the excitation wavelength of 610 nm and therefore to calculate the total concentration of the fluorescing species. In both cases, the yields decrease with increasing sensitizer concentration.

3.1.2. Time-resolved measurements

The decay times and relative amplitudes of AlPcCl in SUVs and LUVs analysed by sum of exponentials (SOE) analysis are given in Table 2 and Table 3 respectively. In both cases, biexponential decays are observed with decay times of approximately 6.8 ns, whose yield decreases with increasing phthalocyanine concentration, and approximately 1.5 ns, whose yield increases with increasing phthalocyanine concentration. The decays were also analysed using global analysis which yielded two decay times of 6.7 and 2.5 ns for AlPcCl in SUVs. The yield of the 6.7 ns decay time decreased with increasing phthalocyanine concentration, whereas the 2.5 ns decay time increased. A similar effect was observed for AlPcCl in LUVs, with the global analysis yielding two decay times of 7.1 ns, whose yield decreased, and 4.1 ns, whose yield increased with increasing sensitizer concentration. A decay time distribution analysis was also applied to the fluorescence decays of AlPcCl in LUVs. The results obtained for phthalocyanine concentrations of 1.0, 4.3 and 12.0 μM are shown in Fig. 4, together with the results obtained from application of this analysis to the corresponding simulated decays.

Table 2
Fluorescence decay times τ_i of AlPcCl in SUVs analysed by SOE analysis

[AlPcCl] (μM)	τ_1 (ns) (A_1 (%))	τ_2 (ns) (A_2 (%))	χ^2	DW [a]
0.30	6.8 (96)	1.0 (4)	1.017	1.82
0.35	6.9 (94)	1.4 (6)	1.095	2.02
0.83	7.1 (79)	2.7 (21)	1.060	2.04
1.45	6.0 (75)	1.4 (25)	1.069	1.62
4.0	6.0 (71)	1.5 (29)	1.088	1.59
5.4	6.1 (67)	1.4 (33)	1.233	1.99
7.2	6.4 (75)	1.8 (25)	1.163	2.13

[a] Durbin–Watson parameter.

Table 3
Fluorescence decay times τ_i of AlPcCl in LUVs analysed by SOE analysis

[AlPcCl] (μM)	τ_1 (ns) (A_1 (%))	τ_2 (ns) (A_2 (%))	χ^2	DW [a]
0.87	6.9 (95)	1.3 (5)	0.979	2.12
1.0	6.9 (94)	1.5 (6)	1.089	2.01
2.7	7.0 (84)	1.9 (16)	1.135	1.94
4.3	6.4 (81)	1.5 (19)	1.019	2.05
6.3	6.9 (79)	1.6 (21)	1.211	2.14
9.0	6.6 (74)	1.7 (26)	1.445	2.01
12.0	6.1 (57)	2.2 (24), τ_3 = 0.4 (19)	1.135	1.85

[a] Durbin–Watson parameter.

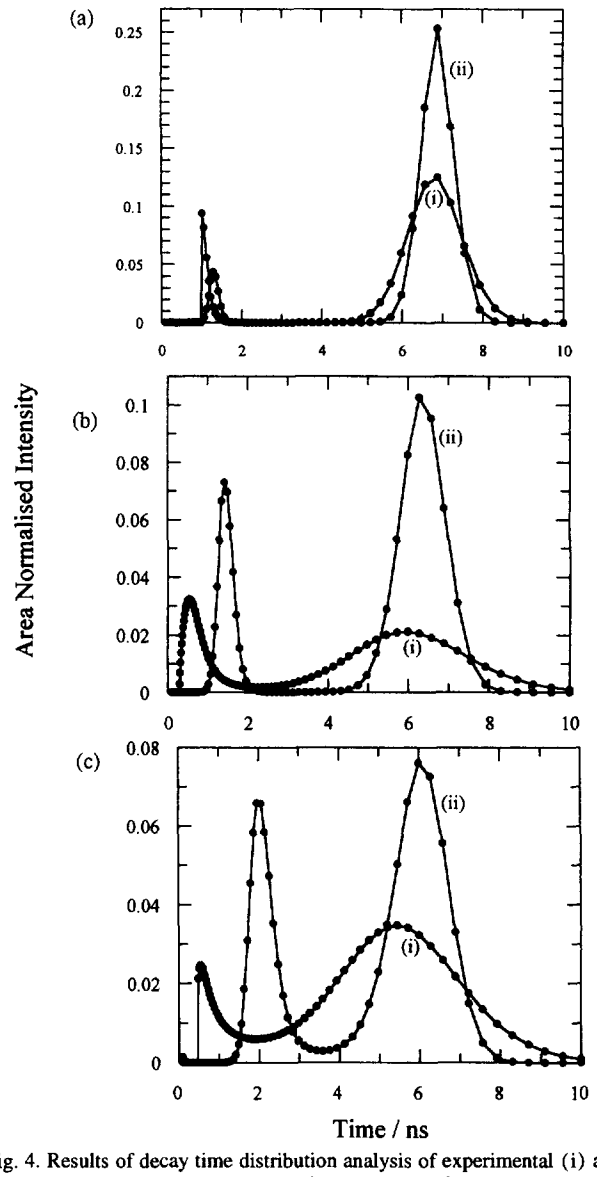

Fig. 4. Results of decay time distribution analysis of experimental (i) and simulated (ii) decays of (a) 1.0×10^{-6}, (b) 4.3×10^{-6} and (c) 12.0×10^{-6} mol dm^{-3} AlPcCl in LUVs.

3.2. cis-$AlPcS_2$ in small and large unilamellar vesicles

3.2.1. Steady state measurements

The absorption spectra of *cis*-$AlPcS_2$ in SUVs and LUVs are shown in Fig. 5 and Fig. 6 respectively. Deviation from linearity in the Beer–Lambert plot in the SUVs (see Fig. 7) indicates the possibility of aggregation. The Beer–Lambert plot for *cis*-$AlPcS_2$ in LUVs, on the other hand, is linear over the entire concentration range, yielding an extinction coefficient of 1.4×10^5 mol^{-1} dm^3. As with AlPcCl, the fluorescence quantum yields decrease with increasing sensitizer concentration in both the SUVs and LUVs. These values are given in Table 4.

3.2.2. Time-resolved measurements

The results obtained from SOE analysis of the fluorescence decay of *cis*-$AlPcS_2$ in SUVs are given in Table 5. The corresponding data obtained for *cis*-$AlPcS_2$ in LUVs are given

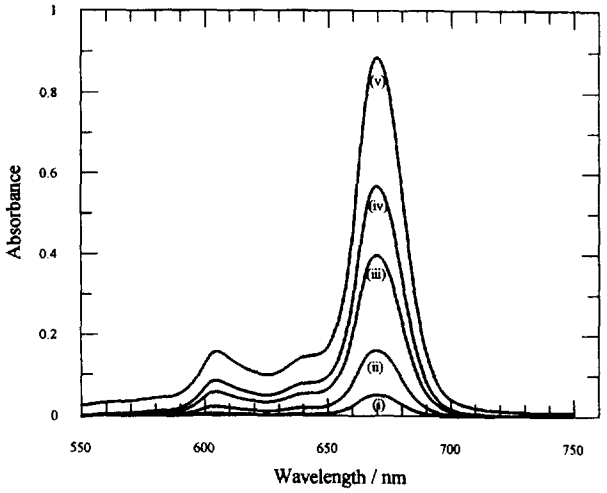

Fig. 5. Absorption spectra of *cis*-$AlPcS_2$ in SUVs at sensitizer concentrations of (i) 0.25×10^{-6}, (ii) 1.01×10^{-6}, (iii) 2.7×10^{-6}, (iv) 4.0×10^{-6} and (v) 7.0×10^{-6} mol dm^{-3}.

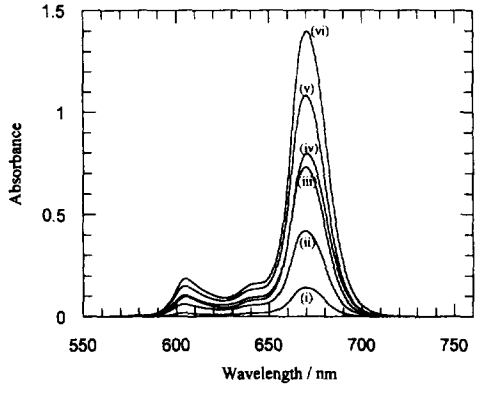

Fig. 6. Absorption spectra of *cis*-$AlPcS_2$ in LUVs at sensitizer concentrations of (i) 0.76×10^{-6}, (ii) 3.0×10^{-6}, (iii) 5.5×10^{-6}, (iv) 8.2×10^{-6}, (v) 10.5×10^{-6} and (vi) 12.2×10^{-6} mol dm^{-3}.

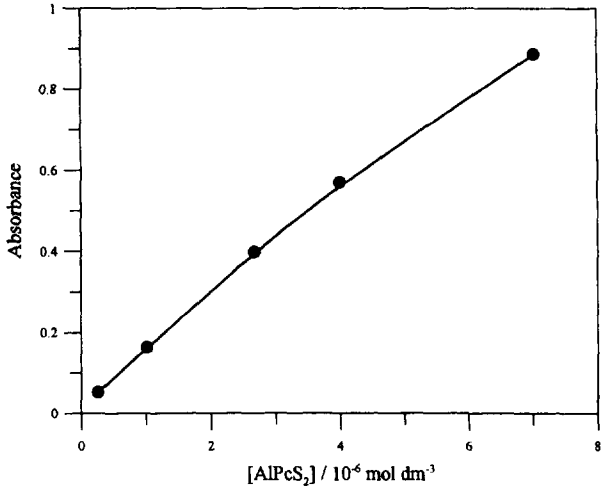

Fig. 7. Variation in the maximum absorbance (673 nm) as a function of the stoichiometric *cis*-$AlPcS_2$ concentration in aqueous dispersions of DPPC SUVs.

in Table 6. In both cases, biexponential decays are obtained. The longer decay time of approximately 6.6 ns at the lower phthalocyanine concentrations decreases gradually to approximately 5 ns as the phthalocyanine concentration is increased, with a corresponding decrease in the yield. The second component remains constant at approximately 1.5 ns at all phthalocyanine concentrations, but its yield increases with increasing sensitizer concentration. The results obtained from the decay time distribution analysis of these decays at *cis*-$AlPcS_2$ concentrations of 2.7, 4.0 and 7.0 μM in SUVs are shown in Fig. 8, together with the results obtained from application of this analysis to the corresponding simulated decays.

Table 4
Fluorescence (Φ_f), triplet (Φ_t) and internal conversion (Φ_{ic}) quantum yields of *cis*-$AlPcS_2$ in DPPC SUVs

[*cis*-$AlPcS_2$] (μM)	Φ_f^a	Φ_t	Φ_{ic}
0.25	0.59	0.59	0.21
1.01	0.42	0.42	0.44
2.67	0.30	0.30	0.58
4.00	0.28	0.28	0.62
7.03	0.23	0.23	0.68

[a] Φ_f not corrected for any dimer/aggregate absorption at the excitation wavelength (610 nm).

Table 5
Fluorescence decay times τ_i of *cis*-$AlPcS_2$ in SUVs analysed by SOE analysis

[*cis*-$AlPcS_2$] (μM)	τ_1 (ns) (A_1 (%))	τ_2 (ns) (A_2 (%))	χ^2	DW [a]
0.25	6.6 (92)	1.0 (8)	1.248	2.01
1.01	6.2 (89)	1.1 (11)	1.212	2.03
2.7	5.4 (81)	1.4 (19)	1.108	2.02
4.0	5.2 (80)	1.3 (20)	1.117	2.30
7.0	5.2 (55)	1.8 (25), τ_3 = 0.58 (20)	1.135	1.80

[a] Durbin–Watson parameter.

Table 6
Fluorescence decay times (τ_i) of *cis*-$AlPcS_2$ in LUVs analysed by SOE analysis

[*cis*-$AlPcS_2$] (μM)	τ_1 (ns)	A_1 (%)	τ_2 (ns)	A_2 (%)	χ^2
0.76	6.8	93	2.0	7	1.16
3.0	6.2	87	1.4	13	1.38
5.5	5.7	80	1.6	20	1.23
8.2	5.2	69	1.6	31	1.33
10.5	4.8	53	1.4	47	1.28

3.3. Physical parameters

The number of phospholipid molecules per liposome is as follows: LUVs, 60 670; SUVs, 25 340.

For LUVs, the concentration of vesicles is 2.6×10^{-8} M. The [sensitizer]:[lipid] ratio is 1:3000 at [sensitizer] = 0.5 μM and 1:133 at [sensitizer] = 12 μM.

Using the Poisson distribution, there will be approximately 15–25 sensitizer molecules per liposome (if [sensitizer]

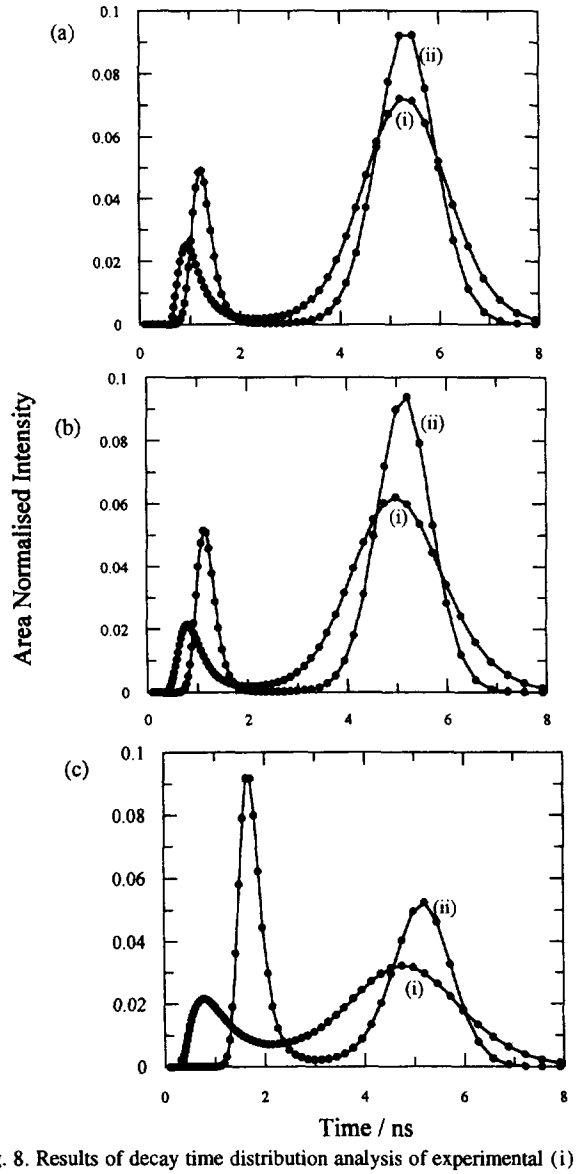

Fig. 8. Results of decay time distribution analysis of experimental (i) and simulated (ii) decays of (a) 2.7×10^{-6}, (b) 4.0×10^{-6} and (c) 7.0×10^{-6} mol dm^{-3} *cis*-$AlPcS_2$ in SUVs.

$=0.5$ μM and [vesicles] $=2.6\times10^{-8}$ M for LUVs). The probability of having two sensitizer molecules together is zero, i.e. [sensitizer]:[lipid] = 1:3333. It has been shown that, if the [sensitizer]:[lipid] ratio is at least 1:1000, the probability of aggregation is zero [23]. For example, no excimer is observed for pyrene in DPPC liposomes when the [sensitizer]:[lipid] ratio is less than 1:100 [23] ([sensitizer] refers to the stoichiometric concentration, i.e. the concentration corresponding to a homogeneous distribution of the phthalocyanine in the entire volume of the liposomal dispersion).

This may explain why aggregation is not observed for *cis*-$AlPcS_2$. On the other hand, a hydrophobic sensitizer, such as AlPcCl, will be confined within the phospholipid bilayer of the aqueous liposomal dispersion. Therefore the volume actually available to it will only be a small fraction of the whole medium and, as a consequence, the motility of the phthalocyanine in the hydrocarbon-type milieu will be severely restricted and the local concentration of the phthalocyanine in the bilayer will be orders of magnitude larger than the stoichiometric concentration, resulting in aggregation.

4. Discussion

A major difference observed between the decay times of AlPcCl and *cis*-$AlPcS_2$ is that, in the *cis*-$AlPcS_2$ system, the longer decay time actually decreases as the phthalocyanine concentration is increased in the vesicles, whereas for AlPcCl both decay times remain constant. The decay time of approximately 6.6 ns at low *cis*-$AlPcS_2$ concentrations indicates that *cis*-$AlPcS_2$ is located in a non-polar environment, probably the hydrocarbon-type milieu of the bilayer. This decay time decreases to approximately 5 ns with increasing phthalocyanine concentration, indicating that the phthalocyanine is in a predominantly aqueous environment. The decay time distributions of *cis*-$AlPcS_2$ broaden with increasing phthalocyanine concentration, indicating that the decay times extracted from SOE analysis are average parameters only. The deviation of the decay time distributions from those of the simulated decays increases progressively for both SUVs and LUVs as the phthalocyanine concentration within the vesicles is increased.

The rate constants of fluorescence k_f, intersystem crossing k_{isc} and internal conversion k_{ic} for *cis*-$AlPcS_2$ in LUVs are given in Table 7. The values of k_f are approximately constant with increasing sensitizer concentration, whereas the values of k_{isc} decrease slightly. The rate constant of internal conversion k_{ic}, on the other hand, increases dramatically with

Table 7
Quantum yields (Φ_x) and rate constants of fluorescence k_f, intersystem crossing k_{isc} and internal conversion k_{ic} for *cis*-$AlPcS_2$ in LUVs

[*cis*-$AlPcS_2$] (μM)	Φ_f^a	Φ_t	Φ_{ic}	k_f (10^7 s^{-1})	k_{isc} (10^7 s^{-1})	k_{ic} (10^7 s^{-1})
0.76	0.48	0.24	0.28	9.14	4.57	5.33
3.04	0.41	0.19	0.40	10.0	4.65	9.78
5.51	0.37	0.17	0.46	8.79	4.04	10.9
8.17	0.30	0.11	0.59	8.15	2.99	16.0
10.45	0.26	0.06	0.68	7.95	1.83	20.8
12.2	0.23	0.04	0.73	7.88	1.37	25.0

[a] Φ_f not corrected for any dimer/aggregate absorption at the excitation wavelength (610 nm).

increasing sensitizer concentration. This result, together with the observed broadening of the decay times, indicates the possibility of there being two locations for the phthalocyanine within the vesicles. At low phthalocyanine concentrations, the phthalocyanine will reside predominantly within the lipid core of the bilayer with only the sulphonate groups exposed to the aqueous phase. As the phthalocyanine concentration is increased, some of the phthalocyanine molecules may be distributed in a second environment, which is in closer proximity to the aqueous phase, resulting in hydration of the central aluminium ion in the phthalocyanine and a reduction in the decay time to approximately 5 ns. The phthalocyanine molecule located in this second environment may also experience an increase in its vibrational degree of freedom as it is not as restricted in its movement due to the greater extent of localization in the aqueous phase. This may explain the marked increase in the rate of internal conversion with increasing sensitizer concentration.

The biexponential decays are not due to the presence of two locations for the phthalocyanine molecules, as the decay time for the molecules in the hydrocarbon-type milieu is approximately 6.5 ns and the decay time for the molecules closer to the aqueous phase is approximately 5 ns. However, the biexponential decays yield a short decay component of approximately 1.5 ns. It is probable that this decay time results from interactions between proximate phthalocyanine molecules. It is evident from this and previous studies [24] that the 1.5 ns decay time is not due to dimer or aggregate fluorescence as the same effects are observed in the non-aggregating microheterogeneous systems. This second decay time is also not due to the location of the phthalocyanine in a different environment in the microheterogeneous system as it has already been established that the two environments produce decay times of approximately 6.5 ns and 5.0 ns depending on the nature of the ligand attached to the central aluminium ion. Therefore this shorter component, which has been observed in several microheterogeneous systems [24,25], seems to be the result of parametrization of a complex decay, and may be caused by the interaction of proximate phthalocyanine rings, resulting in phenomena such as self-quenching or electron transfer. This would explain the increase in the yield of the short decay time with increasing phthalocyanine concentration. Total self-quenching is not observed as there is a distribution of phthalocyanine within the microheterogeneous system. A simplified view is that this distribution consists of regions in which the phthalocyanine is totally isolated (resulting in a decay time of approximately 5–6 ns) and other regions in which proximate phthalocyanine pairs exist (resulting in fluorescence quenching and a shorter decay time). The true picture, however, is probably much more complicated, consisting of a heterogeneous distribution of the fluorophore within the vesicles. Some exciton interaction will occur between these quenching pairs, but no exciton splitting is observed as the separation between the molecules is too large. Such an interaction has been observed for "statistical pairs" in chlorophyll systems [26] and results in a shift in the wavelength of maximum absorption. In this study, a red shift was observed (Fig. 6) which increased with increasing phthalocyanine concentration in the vesicles. The elucidation of the exact mechanism of this interaction requires further study.

A time-resolved fluorescence study carried out by Valduga et al. [10] on zinc(II) phthalocyanine in liposomes also gave multiexponential decays. Quenching studies using external aqueous quenchers indicated that there were at least two populations of liposome-bound phthalocyanine, one accessible and the other(s) inaccessible to aqueous quenchers. However, the multiexponential decays were not the result of a heterogeneous distribution of sensitizer within the vesicles, as the same quenching effect was observed at low phthalocyanine concentrations where the fluorescence decays were monoexponential. The shorter decay times were proposed to be due to either aggregated derivatives or different types of electronic interactions between the π-electron clouds of phthalocyanine molecules having different mutual orientations in the phospholipid bilayer. As mentioned previously, the high local sensitizer concentrations will enhance the probability of intermolecular interactions.

The decay time distribution for the highest concentration of *cis*-$AlPcS_2$ in SUVs is almost continuous, rather than resolved into two bands as observed for the lower phthalocyanine concentrations. This effect is more pronounced in the decay time distributions of AlPcCl in LUVs, occurring at even the lowest concentration. There is also poor agreement between the decay time distributions obtained from the experimental and simulated decays at all AlPcCl concentrations. The "non-resolved" bands in the decay time distributions only occur in systems in which the phthalocyanine is observed to aggregate. Although the dimer/aggregate is non-fluorescent, it exerts an influence on the overall behaviour of the phthalocyanine–vesicle system. The fluorescence decays are more complex for the aggregating systems, and the overall triplet and fluorescence quantum yields decrease. This effect on the quantum yields is also observed in homogeneous systems where the phthalocyanine aggregates and may be caused by energy transfer from the excited state of the monomer to the aggregate, thus enhancing the relaxation of the excited state via the vibrational process of internal conversion. These observations provide further justification for the use of a non-aggregating sensitizer, such as *cis*-$AlPcS_2$, in PDT.

5. Conclusions

The increase in the rate of internal conversion and the broadening of the decay time distributions with increasing *cis*-$AlPcS_2$ concentration in LUVs indicate the possibility of two locations for the phthalocyanine within the vesicles. The fluorescence decay times of the phthalocyanine in these two locations are approximately 6.5 ns and 5.0 ns, depending on the proximity of the phthalocyanine to the aqueous phase and thus the nature of the ligand attached to the central metal.

SOE analysis gives average parameters only and does not separate these two decay times. However, it is evident from the decay time distributions that a distribution of decay times between approximately 5 and 6.5 ns exists. Therefore there may be a number of different locations in microheterogeneous media.

The biexponential decays obtained from SOE analysis of the 5–6.5 ns and 1.5 ns decay times are not due to dimer or aggregate emission as they are observed in both the aggregating and non-aggregating systems. The short decay time of approximately 1.5 ns is believed to be the result of parametrization of a complex decay and is probably due to the interaction of closely located phthalocyanine molecules. The probability of intermolecular interactions will be enhanced at the high local sensitizer concentrations expected in such systems. Although the phthalocyanine aggregate is non-fluorescent, it is still believed to exert an influence on the photophysical behaviour of the phthalocyanine monomer. The overall effect is to increase the complexity of the relaxation mechanisms of the excited state of the sensitizer, resulting in a decrease in the fluorescence and triplet quantum yields. Therefore the photodynamic activity of an aggregated sensitizer is expected to be less than that of a non-aggregating sensitizer, such as *cis*-$AlPcS_2$.

Acknowledgements

We wish to thank British Petroleum for awarding a studentship to S.D. We also wish to acknowledge the SERC Laser Support Facility, Rutherford Appleton Laboratory and Dr. L. Giorgi for the use of equipment.

References

[1] W.-S. Chan, R. Svensen, D. Phillips and I.R. Hart, *Br. J. Cancer, 53* (1986) 255–263.
[2] C.R.J. Singer, D.C. Linch, S.G. Bown, E.R. Huehns and A.H. Goldstone, *Br. J. Haematology, 68* (1988) 417–422.
[3] W.-S. Chan, J.F. Marshall, R. Svensen, J. Bedwell and I.R. Hart, *Cancer Res., 50* (1990) 4533–4538.
[4] M.S. Patterson, B.C. Wilson and R. Graff, *Photochem. Photobiol., 51* (1990) 343–349.
[5] P.T. Chatlani, J. Bedwell, A.J. MacRobert, H. Barr, P.B. Boulos, N. Krasner, D. Phillips and S.G. Bown, *Photochem. Photobiol., 53* (1991) 745–751.
[6] M.A.J. Rodgers, in G. Jori and C. Perria (eds.), *Photodynamic Therapy of Tumours and Other Diseases*, Libreria, Progetto Editore, Padova, 1985, pp. 22–35.
[7] J.E. van Lier and J.D. Spikes, in *Photosensitizing Compounds: Their Chemistry, Biology and Clinical Use*, Ciba Foundation Symposium 146, Wiley, Chichester, 1989.
[8] G. Valduga, S. Nonell, E. Reddi, G. Jori and S.E. Braslavsky, *Photochem. Photobiol., 48* (1988) 1–5.
[9] G. Valduga, E. Reddi and G. Jori, *J. Inorg. Biochem., 29* (1987) 59–65.
[10] G. Valduga, E. Reddi, G. Jori, R. Cubeddu, P. Taroni and G. Valentini, *J. Photochem. Photobiol. B: Biol., 16* (1992) 331–340.
[11] M. Ambroz, A. Beeby, A.J. MacRobert, M.S.C. Simpson, R.K. Svenson and D. Phillips, *J. Photochem. Photobiol. B: Biol., 9* (1991) 87–95.
[12] S.M. Bishop, A. Beeby, A.J. MacRobert, B.J. Khoo, M.S.C. Simpson and D. Phillips, *J. Chromatogr., 646* (1993) 345–350.
[13] J.M.H. Kremer, M.W.J. von der Esker, C. Pathmamanoharan and P.H. Wirsma, *Biochemistry, 16* (1977) 3932–3955.
[14] A.D. Bangham, M.H. Standish and J.C. Watkins, *J. Mol. Biol. B, 13* (1965) 238–252.
[15] S. Dhami, A.J. DeMello, G. Rumbles, S.M. Bishop, D. Phillips and A. Beeby, *Photochem. Photobiol., 61* (1995) 341–346.
[16] G. Weber and J.W.F. Teale, *Trans. Faraday Soc., 53* (1957) 646.
[17] A. Beeby, S.M. Bishop, H.G. Meunier, M.S.C. Simpson and D. Phillips, in P. Spinelli, M. Dal Fante and R. Marchesini (eds.), *Photodynamic Therapy and Biomedical Lasers*, Elsevier Science, 1992.
[18] D. Phillips and D.V. O'Connor, in *Time-Correlated Single-Photon Counting*, Academic Press, London, 1984.
[19] J.R. Knutsen, J.M. Beecham and L. Brand, *Chem. Phys. Lett., 102* (1983) 501.
[20] A. Siemiarczuk and W.R. Ware, *Chem. Phys. Lett., 160* (1989) 285–290.
[21] A. Beeby, A.W. Parker and D. Phillips, in *SERC—The Rutherford Appleton Laboratory Central Laser Facility Annual Report*, 1991, pp. 193–195.
[22] S.M. Bishop, Preparation and properties of phthalocyanine sensitisers for photodynamic therapy (PDT), *Ph.D. Thesis*, University of London, 1993.
[23] C.D. Borsarelli, J.J. Cosa and C.M. Previtali, *Langmuir, 9* (11) (1993) 2895–2901.
[24] S. Dhami, J.J. Cosa, S.M. Bishop and D. Phillips, *Langmuir, 12* (2) (1996) 293–300.
[25] M. Ambroz, A.J. MacRobert, J. Morgan, G. Rumbles, M.S.C. Foley and D. Phillips, *J. Photochem. Photobiol. B: Biol., 22* (1994) 105–117.
[26] R.S. Knox, *J. Phys. Chem., 98* (1994) 7270–7273.